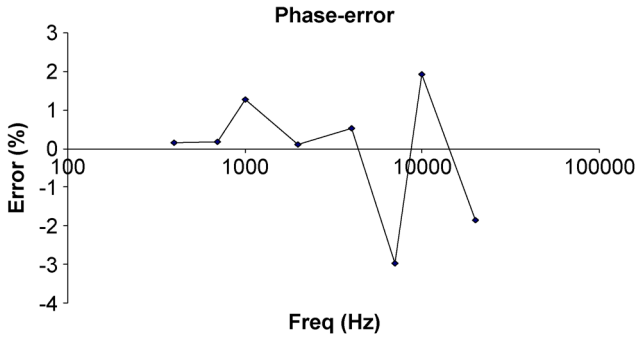

Fig. 3. Phase error with frequency.

results are very close to reality because of the simplicity of the bridge-balance technique. The percentage errors of k and ψ are plotted against frequency in the range of 100 Hz to 70 kHz in Figs. 2 and 3, respectively. The phase error curve has more errors because of field noise. The efficiency of the measurement can be improved by increasing the resolution and the sampling rate of the analog-to-digital converter (ADC)/DAC. A pair of a 12-bit DAC and a 16-bit 1-mega samples per second ADC has been used. RMS voltages can be an alternative method instead of measuring peak amplitudes of the error signal, but the peak measurement method is for wide frequency applications. In this paper, the proposition aims more to feasibility than to precision. Our aim is to use this development in eddy-current nondestructive test instruments. There are many other applications where this measurement technique can give immense advantages.

IV. Discussions and Conclusion

We have developed an innovative automatic digital ac bridge-balance technique. The technique is found to have a very small error. Adoption of this technique enables miniaturization of instrumentation with high accuracy, and it is giving the balance point over a wide frequency range. In fast breeder nuclear reactors, the eddy-current technique is used in many safety-critical systems. In such cases, the complexity in hardware and software reduces the reliability of the system. To reduce the probability of failure on demand, we need to optimize the complexity of hardware and software. This technique has obtained both minimum hardware and software; therefore, we see that it can be used to a very wide and versatile application in many other fields of measurements.

References

[1] W. Helbach and H. Schollmeyer, "Impedance measuring methods based on multiple digital generators," *IEEE Trans. Instrum. Meas.*, vol. IM-36, no. 2, pp. 400–405, Jun. 1987.

[2] M. Dutta, A. Rakshit, S. N. Bhattyacharyya, and J. K. Choudhury, "An application of the LMS adaptive algorithm for a digital AC bridge," *IEEE Trans. Instrum. Meas.*, vol. IM-36, no. 2, pp. 894–897, Dec. 1987.

[3] S. S. Awad, N. Narasimhamurthi, and W. H. Ward, "Analysis, design and implementation of an AC bridge for impedance measurements," *IEEE Trans. Instrum. Meas.*, vol. 43, no. 6, pp. 894–899, Dec. 1994.

[4] M. Dutta, A. Rakshit, and S. N. Bhattyacharyya, "Development and study of an automatic ac bridge for impedance measurement," *IEEE Trans. Instrum. Meas.*, vol. 50, no. 5, pp. 1048–1052, Oct. 2001.

[5] J. Q. Zhang, S. J. Ovaska, and Z. Xinmim, "A novel fast balance technique for the digital ac bridge," *IEEE Trans. Instrum. Meas.*, vol. 47, no. 2, pp. 371–377, Apr. 1998.

[6] P. Holmberg, "Automatic balancing of linear AC bridge circuits for capacitive sensor elements," *IEEE Trans. Instrum. Meas.*, vol. 44, no. 3, pp. 803–805, Jun. 1995.

[7] N. Hagiwara, M. Yanase, and T. Saegusa, "A self-balance-type capacitance-to-DC-voltage converter for measuring small capacitance," *IEEE Trans. Instrum. Meas.*, vol. IM-36, no. 2, pp. 385–389, Jun. 1987.

[8] B. C. Waltrip and N. M. Oldham, "Digital impedance bridge," *IEEE Trans. Instrum. Meas.*, vol. 44, no. 2, pp. 436–439, Apr. 1995.

[9] A. Muciek, "Digital impedance bridge based on a two-phase generator," *IEEE Trans. Instrum. Meas.*, vol. 46, no. 2, pp. 467–470, Apr. 1997.

[10] A. Carullo, M. Parvis, A. Vallan, and L. Callegaro, "Automatic compensation system for impedance measurement," *IEEE Trans. Instrum. Meas.*, vol. 52, no. 4, pp. 1239–1242, Aug. 2003.

[11] M. Dutta, A. Chatterjee, and A. Rakshit, "Intelligent phase correction in automatic digital ac bridges by resilient backpropagation neural network," *Measurement*, vol. 39, no. 10, pp. 884–891, Dec. 2006.

Digital Image Watermarking Using Discrete Wavelet Transform and Singular Value Decomposition

Chih-Chin Lai, *Member, IEEE*, and Cheng-Chih Tsai

***Abstract*—The main objective of developing an image-watermarking technique is to satisfy both imperceptibility and robustness requirements. To achieve this objective, a hybrid image-watermarking scheme based on discrete wavelet transform (DWT) and singular value decomposition (SVD) is proposed in this paper. In our approach, the watermark is not embedded directly on the wavelet coefficients but rather than on the elements of singular values of the cover image's DWT subbands. Experimental results are provided to illustrate that the proposed approach is able to withstand a variety of image-processing attacks.**

***Index Terms*—Authentication, copyright protection, digital watermarking, discrete wavelet transform (DWT), singular value decomposition (SVD).**

I. Introduction

Owing to the popularity of the Internet and the rapid growth of multimedia technology, users have more and more chances to use multimedia data. Consequently, the protection of the intellectual property rights of digital media has become an urgent issue. Digital watermarking has attracted considerable attention and has numerous applications, including copyright protection, authentication, secret communication, and measurement [1], [2].

According to the domain in which the watermark is inserted, these techniques are classified into two categories, i.e., spatial-domain and transform-domain methods. Embedding the watermark into the spatial-domain component of the original image is a straightforward method. It has the advantages of low complexity and easy implementation. However, the spatial-domain methods are generally fragile to image-processing operations or other attacks. On the other hand, the representative transform-domain techniques embed the watermark by modulating the magnitude of coefficients in a transform domain, such as discrete cosine transform, discrete wavelet transform (DWT), and

Manuscript received April 24, 2010; revised May 21, 2010; accepted May 22, 2010. Date of publication September 2, 2010; date of current version October 13, 2010. This work was supported by the National Science Council, Taiwan, under Grant NSC 98-2221-E-390-027. The Associate Editor coordinating the review process for this paper was Dr. Emil Petriu.

C.-C. Lai is with the Department of Electrical Engineering, National University of Kaohsiung, Kaohsiung 81148, Taiwan (e-mail:cclai@nuk.edu.tw).

C.-C. Tsai is with the Department of Computer Science and Information Engineering, National Taiwan University, Taipei 10617, Taiwan.

Digital Object Identifier 10.1109/TIM.2010.2066770

singular value decomposition (SVD) [3], [4]. Although transform-domain methods can yield more information embedding and more robustness against many common attacks, the computational cost is higher than spatial-domain watermarking methods.

Due to its excellent spatio-frequency localization properties, the DWT is very suitable to identify areas in the cover image where a watermark can be imperceptibly embedded. One of attractive mathematical properties of SVD is that slight variations of singular values do not affect the visual perception of the cover image, which motivates the watermark embedding procedure to achieve better transparency and robustness. Consequently, many image-watermarking techniques combining these two transform methods have been proposed [5]–[8]. For a detailed description on the aforementioned approaches, interested readers may directly refer to them.

Since performing SVD on an image is computationally expensive, this study aims to develop a hybrid DWT-SVD-based watermarking scheme that requires less computation effort to yield better performance. After decomposing the cover image into four subbands by one-level DWT, we apply SVD only to the intermediate frequency subbands and embed the watermark into the singular values of the aforementioned subbands to meet the imperceptibility and robustness requirements. The main properties of this work can be identified as follows: 1) Our approach needs less SVD computation than other methods. 2) Unlike most existing DWT-SVD-based algorithms, which embed singular values of the watermark into the singular values of the cover image, our approach directly embeds the watermark into the singular values of the cover image to better preserve the visual perceptions of images.

II. Background Review and the Proposed Approach

A. DWT

The DWT has received considerable attention in various signal-processing applications, including image watermarking. The main idea behind DWT results from multiresolution analysis [9], which involves decomposition of an image in frequency channels of constant bandwidth on a logarithmic scale. It has advantages such as similarity of data structure with respect to the resolution and available decomposition at any level. The DWT can be implemented as a multistage transformation. An image is decomposed into four subbands denoted LL, LH, HL, and HH at level 1 in the DWT domain, where LH, HL, and HH represent the finest scale wavelet coefficients and LL stands for the coarse-level coefficients. The LL subband can further be decomposed to obtain another level of decomposition. The decomposition process continues on the LL subband until the desired number of levels determined by the application is reached. Since human eyes are much more sensitive to the low-frequency part (the LL subband), the watermark can be embedded in the other three subbands to maintain better image quality.

B. SVD-Based Watermarking

From the perspective of image processing, an image can be viewed as a matrix with nonnegative scalar entries. The SVD of an image A with size $m \times m$ is given by $A = USV^T$, where U and V are orthogonal matrices, and $S = \mathrm{diag}(\lambda_i)$ is a diagonal matrix of singular values λ_i, $i = 1, \ldots, m$, which are arranged in decreasing order. The columns of U are the left singular vectors, whereas the columns of V are the right singular vectors of image A. The basic idea behind the SVD-based watermarking techniques is to find the SVD of the cover image or each block of the cover image, and then modify the singular values to embed the watermark. There are two main properties to employ the SVD method in the digital-watermarking scheme: 1) When a small perturbation is added to an image, large variation of its singular values does not occur. 2) Singular values represent intrinsic algebraic image properties [3].

C. Proposed DWT-SVD Watermarking Scheme

The proposed DWT-SVD watermarking scheme is formulated as given here.

1) Watermark embedding:
   1) Use one-level Haar DWT to decompose the cover image A into four subbands (i.e., LL, LH, HL, and HH).
   2) Apply SVD to LH and HL subbands, i.e.,
   $$A^k = U^k S^k V^{kT}, \qquad k = 1, 2 \tag{1}$$
   where k represents one of two subbands.
   3) Divide the watermark into two parts: $W = W^1 + W^2$, where W^k denotes half of the watermark.
   4) Modify the singular values in HL and LH subbands with half of the watermark image and then apply SVD to them, respectively, i.e.,
   $$S^k + \alpha W^k = U_W^k S_W^k V_W^{kT} \tag{2}$$
   where α denotes the scale factor. The scale factor is used to control the strength of the watermark to be inserted.
   5) Obtain the two sets of modified DWT coefficients, i.e.,
   $$A^{*k} = U^k S_W^k V^{kT}, \qquad k = 1, 2. \tag{3}$$
   6) Obtain the watermarked image A_W by performing the inverse DWT using two sets of modified DWT coefficients and two sets of nonmodified DWT coefficients.
2) Watermark extraction:
   1) Use one-level Haar DWT to decompose the watermarked (possibly distorted) image A_W^* into four subbands: LL, LH, HL, and HH.
   2) Apply SVD to the LH and HL subbands, i.e.,
   $$A_W^{*k} = U^{*k} S_W^{*k} V^{*kT}, \qquad k = 1, 2 \tag{4}$$
   where k represents one of two subbands.
   3) Compute $D^{*k} = U_W^k S_W^{*k} V_W^{kT}$, $k = 1, 2$.
   4) Extract half of the watermark image from each subband, i.e.,
   $$W^{*k} = (D^{*k} - S^k)/\alpha, k = 1, 2. \tag{5}$$
   5) Combine the results of Step 4 to obtain the embedded watermark: $W^* = W^{*1} + W^{*2}$.

III. Experimental Results

Several experiments are presented to demonstrate the performance of the proposed approach. The gray-level images "Lena" of size 256 × 256 and "Cameraman" of size 128 × 128 are used as the cover image and the watermark, respectively. These images are shown in Fig. 1(a) and (b). Fig. 1(c) illustrates the watermarked image. It can be observed that the proposed approach preserves the high perceptual quality of the watermarked image.

As a measure of the quality of a watermarked image, the peak signal-to noise ratio (PSNR) was used. To evaluate the robustness of the proposed approach, the watermarked image was tested against five kinds of attacks: 1) geometrical attack: cropping (CR) and rotation

(a) (b) (c)

Fig. 1. (a) Cover image. (b) Watermark image. (c) Watermarked image (PSNR $= 51.14$).

TABLE I
PEARSON'S CORRELATION COEFFICIENT VALUES OF EXTRACTED WATERMARKS FROM DIFFERENT ATTACKS

SF value	CR	RO	GN	AF
0.01	0.9452	0.9609	0.9415	0.9469
0.03	0.9633	0.9654	0.9394	0.9360
0.05	0.9803	0.9780	0.9591	0.9597
0.07	0.9824	0.9888	0.9720	0.9511
0.09	0.9843	0.9898	0.9756	0.9417
SF value	JPEG	HE	CA	GC
0.01	0.9509	0.9803	0.9862	0.9807
0.03	0.9605	0.9860	0.9929	0.9965
0.05	0.9772	0.9862	0.9936	0.9982
0.07	0.9679	0.9888	0.9951	0.9992
0.09	0.9704	0.9890	0.9958	0.9994

TABLE II
COMPARISON OF IMPERCEPTIBILITY (PSNR) FOR G&E [7], L&T [3], AND OUR ALGORITHM

SF value	0.01	0.03	0.05	0.07	0.09
G&E [7]	37.80	36.79	35.29	33.72	32.26
L&T [3]	51.50	51.26	50.05	47.84	45.56
Ours	51.14	51.14	50.89	49.52	47.49

(RO); 2) noising attack: Gaussian noise (GN); 3) denoising attack: average filtering (AF); 4) format-compression attack: JPEG compression; and 5) image-processing attack: histogram equalization (HE), contrast adjustment (CA), and gamma correction (GC). For comparing the similarities between the original and extracted watermarks, the Pearson's correlation coefficient was employed. In the experiments, the values of the scale factors are carried out with constant range from 0.01 to 0.09 with an interval of 0.02, and the results are illustrated in Tables I and II. It can be seen that the larger the scale factor, the stronger the robustness of the applied watermarking scheme. In contrast, the smaller the scale factor, the better the image quality.

In order to justify our approach, we also implement the DWT-SVD-based watermarking method [7] and pure SVD-based approach [3] to compare the performance. The adjustment strategy of scale factors is like our aforementioned experiment setting, and experimental results are listed in Tables II and III. After studying the experimental results, it can be seen that the proposed scheme significantly outperforms the two compared schemes. In addition to quantitative measurement, we also need the visual perceptions of the extracted watermarks. The constructed watermarks with best-quality measurement are shown in Fig. 2(a)–(x), and we can find that our scheme not only can successfully resist different kinds of attacks but can also restore watermark with high perceptual quality.

To compare the efficiency of our approach and other two methods, watermark extraction was performed on nonattacked watermarked images using the three methods. We implemented three watermarking schemes using C# and ran them on a personal computer with Intel

TABLE III
COMPARISON OF ROBUSTNESS FOR G&E [7], L&T [3], AND OUR ALGORITHM

	CR		RO		GN	
Method	Best	Average	Best	Average	Best	Average
G&E [7]	0.7063	0.2798	0.9091	0.8843	0.9377	0.9169
L&T [3]	0.9578	0.9412	0.9444	0.9394	0.8953	0.8857
Ours	0.9843	0.9728	0.9897	0.9772	0.9756	0.9567
	AF		JPEG		HE	
Method	Best	Average	Best	Average	Best	Average
G&E [7]	-0.7047	-0.8172	0.9226	0.7537	0.9700	0.9498
L&T [3]	0.8978	0.8765	0.9554	0.9356	0.9780	0.9761
Ours	0.9597	0.9500	0.9772	0.9658	0.9890	0.9862
	CA		GC			
Method	Best	Average	Best	Average		
G&E [7]	0.9759	0.9544	0.9989	0.9927		
L&T [3]	0.9848	0.9827	0.9871	0.9764		
Ours	0.9958	0.9930	0.9994	0.9957		

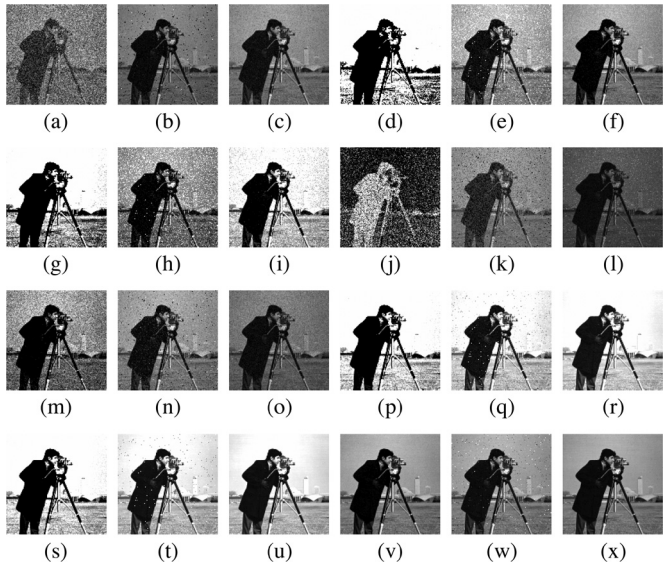

(a) (b) (c) (d) (e) (f)
(g) (h) (i) (j) (k) (l)
(m) (n) (o) (p) (q) (r)
(s) (t) (u) (v) (w) (x)

Fig. 2. Extracted watermarks obtained from G&E [7], L&T [3], and our approach in that order with different attacks: CR[(a)–(c)], RO[(d)–(f)], GN[(g)–(i)], AF[(j)–(l)], JPEG[(m)–(o)], HE[(p)–(r)], CA[(s)–(u)], and GC[(v)–(x)].

TABLE IV
COMPARISON OF EFFICIENCY FOR G&E [7], L&T [3], AND OUR ALGORITHM (UNIT: SECONDS)

	G&E [7]	L&T [3]	Ours
watermark embedding	2.989	5.710	2.107
watermark extraction	2.301	3.964	1.086

Core 2 Duo Processors rated at 2.13 GHz, main memory of 4 GB, and operating system of Microsoft Windows 7. Experimental results are listed in Table IV. It is clearly observed that our method can be done very efficiently in comparison with other existing watermarking schemes.

IV. CONCLUSION

In this paper, a hybrid image-watermarking technique based on DWT and SVD has been presented, where the watermark is embedded on the singular values of the cover image's DWT subbands. The technique fully exploits the respective feature of these two transform-domain methods: spatio-frequency localization of DWT and SVD

efficiently represents intrinsic algebraic properties of an image. Experimental results of the proposed technique have shown both the significant improvement in imperceptibility and the robustness under attacks. Further work of integrating the human visual system characteristics into our approach is in progress.

REFERENCES

[1] J. Sang and M. S. Alam, "Fragility and robustness of binary-phase-only-filter-based fragile/semifragile digital image watermarking," *IEEE Trans. Instrum. Meas.*, vol. 57, no. 3, pp. 595–606, Mar. 2008.

[2] H.-T. Wu and Y.-M. Cheung, "Reversible watermarking by modulation and security enhancement," *IEEE Trans. Instrum. Meas.*, vol. 59, no. 1, pp. 221–228, Jan. 2010.

[3] R. Liu and T. Tan, "An SVD-based watermarking scheme for protecting rightful ownership," *IEEE Trans. Multimedia*, vol. 4, no. 1, pp. 121–128, Mar. 2002.

[4] A. Nikolaidis and I. Pitas, "Asymptotically optimal detection for additive watermarking in the DCT and DWT domains," *IEEE Trans. Image Process.*, vol. 12, no. 5, pp. 563–571, May 2003.

[5] V. Aslantas, L. A. Dogăn, and S. Ozturk, "DWT-SVD based image watermarking using particle swarm optimizer," in *Proc. IEEE Int. Conf. Multimedia Expo*, Hannover, Germany, 2008, pp. 241–244.

[6] G. Bhatnagar and B. Raman, "A new robust reference watermarking scheme based on DWT-SVD," *Comput. Standards Interfaces*, vol. 31, no. 5, pp. 1002–1013, Sep. 2009.

[7] E. Ganic and A. M. Eskicioglu, "Robust DWT-SVD domain image watermarking: Embedding data in all frequencies," in *Proc. Workshop Multimedia Security*, Magdeburg, Germany, 2004, pp. 166–174.

[8] Q. Li, C. Yuan, and Y.-Z. Zhong, "Adaptive DWT-SVD domain image watermarking using human visual model," in *Proc. 9th Int. Conf. Adv. Commun. Technol.*, Gangwon-Do, South Korea, 2007, pp. 1947–1951.

[9] S. Mallat, "The theory for multiresolution signal decomposition: The wavelet representation," *IEEE Trans. Pattern Anal. Mach. Intell.*, vol. 11, no. 7, pp. 654–693, Jul. 1989.